The Influence of Vent Setting on Salt Spray Dissipating in the Longitudinal Beam of Piled Beam-slab Wharfs

Ning Zhuang[1]*, Honghan Dong[1], Xinkai Li[2] and Yeming Ma[1]

[1]College of Harbor, Coastal and Offshore Engineering, Hohai University, Nanjing 210098, China
[2]School of River and Ocean Engineering, Chongqing Jiaotong University, Chongqing 400074, China

*Corresponding author email: 1037158873@qq.com

Abstract. The salt spray gathering in the grillage space of piled beam-slab wharf could easily make the beams corroded in the harsh marine environment, which would cause an adverse impact on the durability of structure. The three dimension model of grillage space of piled beam-slab wharf was established by the fluid dynamic module CFD of ANSYS. Based on the results the vent setting was optimized, the result showed that the vent setting in the longitudinal beam could improve air flow distribution of grillage space effectively. As the distance between the vent and two ends of beam was about one meter, the dissipation effects for salt spray was most significant.

1. Introduction

The beam-slab wharf has been widely used in coastal port engineering in China due to its strong bearing capacity and environmental application ability. The crossbeams are usually interleaved and form the grillage under the dock panel. A lot of salt mist and moist air will gather in the beam space and accelerate the corrosion speed of the vertical and horizontal beam. This phenomenon will cause adverse effect to the durability of wharf structures.

At present, research on the durability of high pile wharf mainly focused on how to improve the durability of building materials themselves. For example, SH Liu, Wei Su [1] etc. studied how to protect steel structures against corrosion using thermal spraying technology. Jing Lu, GH Wang [2] etc. studied how to manufacture anti-corrosion coating material by the cold spray technology. Dr. ZW Jiang [3] etc. from TONGJI University studied the effect on protecting different mix of Marine concrete from corrosion. The corrosive medium mainly consists of the salt mist and moist air accumulated in beam space for the upper structure. Therefore, setting the ventilation hole can avoid reducing durability from the structure itself and save cost to a large degree. This paper will use CFD to explore the effect on distribution of wind field by setting different ventilation holes layout schemes. This has certain innovation significance and practical application value.

2. Application of Ventilation Hole in Engineerings

2.1. General Situation of Engineering Examples

There was severe rust damage about a container terminal in Southern China which belongs to the tropical maritime climate of South Asia. In view of this situation, this paper will analysis the gathering of salt fog by using finite element software ANSYS to build a 3d physical model and determine the optimal layout of ventilation hole. Sectional dimension drawing of high piled wharf is shown in Fig. 1 (unit: mm):

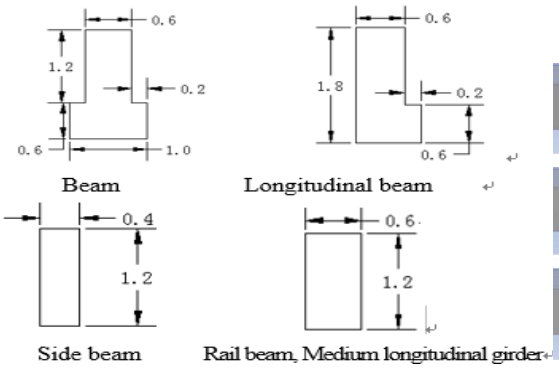

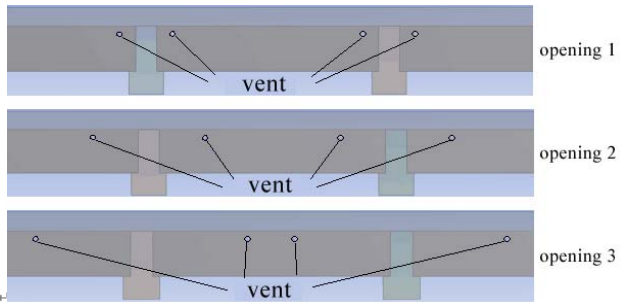

Figure 1. Sectional dimension of beams **Figure 2.** Schematic diagram of ventilation hole layout

2.2. Layout of Ventilation Hole

The vent is arranged on the longitudinal beam. The diameter of it is 12 cm and the wind speed designed is 5/s. The wind direction is designed for vertical longitudinal beam direction. This paper will study the law of movement of internal airflow in grillage space by analyzing the three kinds of layout of ventilation holes [4] (Fig. 2).

Opening 1: Open two holes in the area near the top of the longitudinal beam and upper edge distance from the panel is 15cm, the both ends edges from the beam is 40 cm. Opening 2: Upper edge distance from the panel is 15cm, the both ends edges from the beam is 120 cm. Opening 3: Upper edge distance from the panel is 15cm, the both ends edges distance from the beam is 240 cm. According to the actual situation, the diameter of the drain is set 10 cm and locates at the 1/4 span of the beam direction. Distance from the beam is 1.5 m and only set two drains of a bent diagonally opposite the panel.

3. Mathematical Model and Numerical Simulation

3.1. Governing Equation

Turbulence model K-ξ is suitable for the most engineering turbulence model due to its better university. Among this model, K represents the turbulent kinetic energy that defined a change in velocity (unit: m2/s2). Equation of basic control:

Equation of continuity:

$$\frac{\partial U_i}{\partial X_i} = 0 \tag{1}$$

Equation of momentum:

$$\frac{\partial}{\partial t}(\rho U_i) + \frac{\partial}{\partial X_i}(\rho U_i U_j) = -\frac{\partial P}{\partial X_i} + \frac{\partial}{\partial X_j}\left[\mu \frac{\partial U_i}{\partial X_j} + \mu_t\left(\frac{\partial U_i}{\partial X_j} + \frac{\partial U_j}{\partial X_i}\right)\right] + \rho g + F_i \tag{2}$$

Among them, ρ: fluid density; U_i: velocity component along the i direction; U_j: velocity component along the j direction; μ: coefficient of dynamic viscosity; F_i: body forces acting on the unit mass water body; μ_t: viscosity of a turbulence; Model K-ξ assumed that viscosity of a turbulence is related to dissipation of turbulent kinetic energy, namely:

$$\mu_t = C_\mu \rho \frac{K^2}{\varepsilon} \tag{3}$$

Equation of the urbulent kinetic energy:

$$\frac{\partial}{\partial t}(\rho k) + \frac{\partial}{\partial X_i}(\rho U_i k) = -\frac{\partial}{\partial X_i}\left[(\mu + \frac{\mu_t}{\sigma_k})\frac{\partial k}{\partial X_i}\right] + G - \rho\varepsilon \tag{4}$$

$$\frac{\partial}{\partial t}(\rho\varepsilon) + \frac{\partial}{\partial X_i}(\rho U_i \varepsilon) = \frac{\partial}{\partial X_i}\left[(\mu + \frac{\mu_t}{\sigma_\varepsilon})\frac{\partial k}{\partial X_j}\right] + C_{\varepsilon_1}\frac{\varepsilon}{k}G - C_{\varepsilon_2}\frac{\varepsilon^2}{k}\rho \tag{5}$$

Among them, Cε1, Cε2, σs: constants. ξ: turbulent dissipation rate. σs: dissipation rating Perirt constant. G: turbulent product of adhesive force and buoyancy. The equation is :

$$G = \mu_t(\frac{\partial U_i}{\partial X_j} + \frac{\partial U_j}{\partial X_i}) \times \frac{\partial U_i}{\partial X_j} \tag{6}$$

X_i, X_j : physical space coordinate. Ui, Uj: velocity component along the i, j direction.

3.2. Solution and Boundary Conditions

The finite volume method is used for discrete computation. The convective term adopts the second order windward format and the pressure velocity coupling adopts SIMPLE algorithm. The calculation boundary conditions: given inlet velocity of flow; the entrance boundary conditions: air inlet; velocity of flow: 5m/s; the type of boundary conditions: inlet, an atm; turbulent intensity: 5%; outlet boundary: presser-outlet; the type of boundary condition: outlet; the boundary of solid wall: no slip wall boundary.

3.3. Determination of the Independence of Grid

When the initial wind speed is set 5m/s, change of air volume in a ventilating hole within different boundary mesh sizes is as the following table 1:

Table 1. Air volume of vent corresponding to different boundary mesh sizes

Boundary grid division(m)	0.1	0.3	0.5	0.7	1.0
Air volume of vent(m3/s)	0.102	0.120	0.174	0.229	0.271

According to the above results, when the size of the grid is 0.1m and 0.3m, the difference of the result is less than 4%. Considering the grid computing, the size of the grid is determined to be 0.3m.

3.4. Numerical Model of the Wharf

The three-dimensional model of the beam-slab wharf beam grillage is as fig.3. The maximum grid size of the mesh reconstruction is set to 0.5m; the iteration interval is set to 2. The vent set at the side beam on the windward side is pressure inlet. The other beam is pressure outlet. The calculation domain is selected as: 1m all around the panel; 3m between the bottom of the panel and the boundary of the computing domain; 1m from the boundary of the top [5].

4. Calculation Results and Analysis

The eight points are chosen as computational feature points. The distribution of the points is as Fig.3.

4.1. Situation of No Vents

Prepare for the optimal placement of the vents by calculating the wind speed, pressure and the concentration of salt fog in the certain beam space. Situation of the wind speed chosen when the speed of the inlet is 5m/s is as Fig.4.

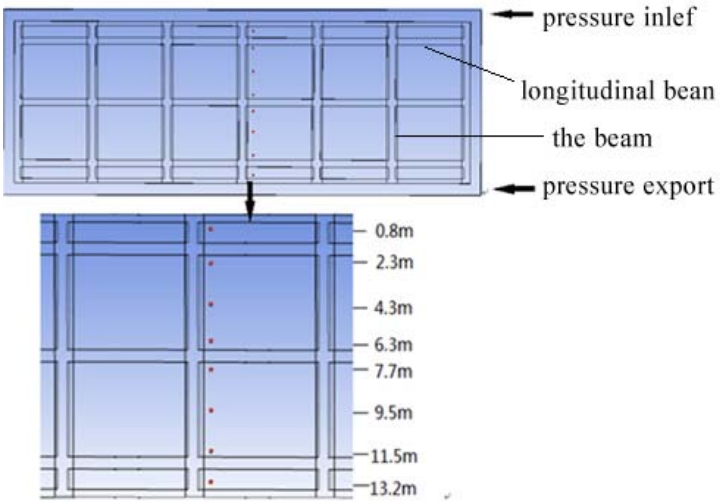

Figure 3. Model of computational feature points

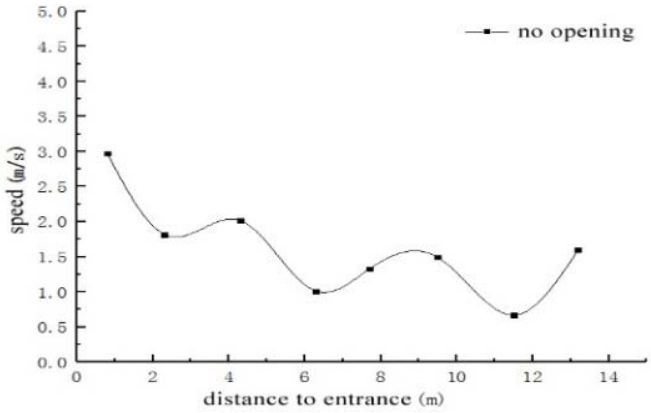

Figure 4. Air velocity distribution of the beam lattice without vents

As the Fig.4 shows, the peak is located at the midpoint of the beam lattice. The trough is close to the entrance side of the longitudinal beam and the middle longitudinal beam. The wind speed is generally lower than 2m/s. This indicates that the certain space is easy gathered salt fog due to weak airflow.

4.2. Transverse Opening of Longitudinal Beam

Setting vents on the longitudinal beam of the high - pile wharf can make the beam lattice more affected by the external air flow. This can form the diversity of natural wind pressure and effectively disperse the salt fog. Velocity vector pictures of three types of opening methods are as Fig.5.

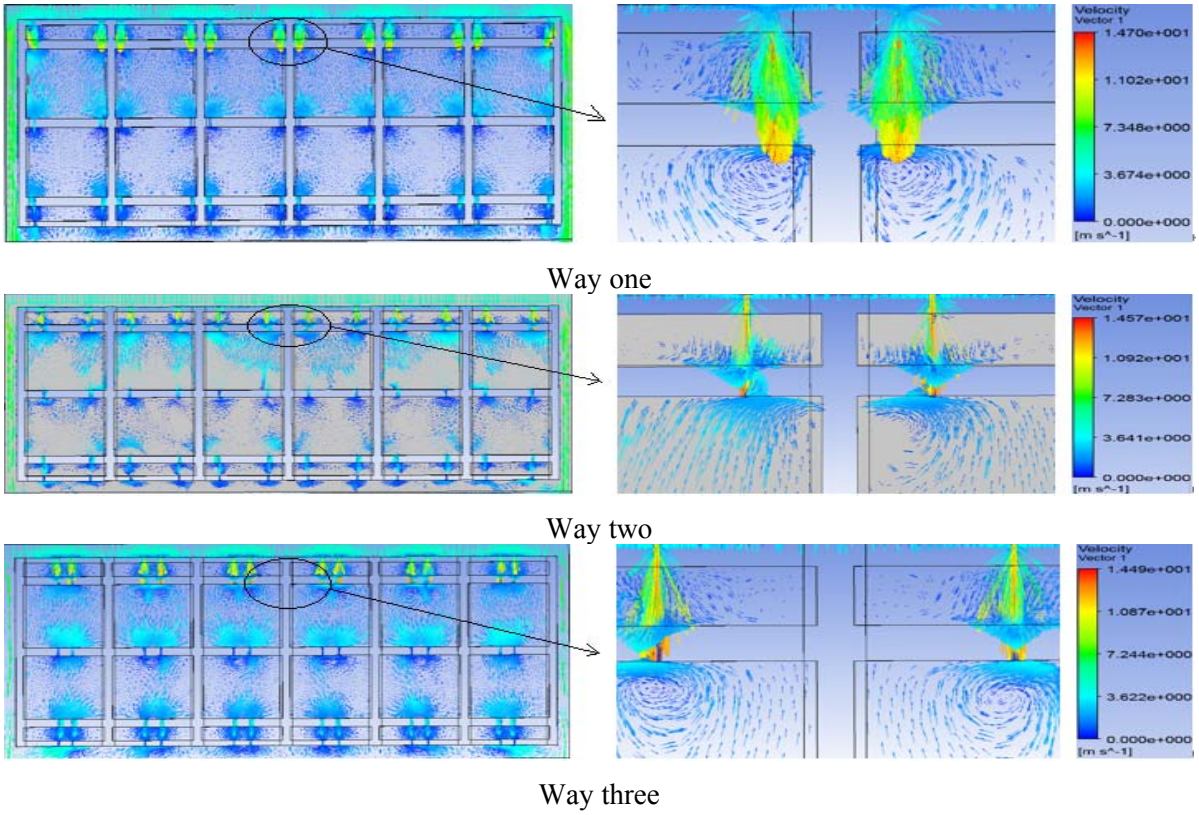

Figure 5. Velocity vector pictures of the beam lattice of three opening ways

As the Fig.5 shows, airflow turbulence around the vents is strong when the wind is blowing directly to the land. At the entrance, the airflow is dense and the wind speed is large side the longitudinal beam and track beam near the vents. The wind speed is relatively weak from the middle longitudinal beam to the exit. However, there are still relatively strong disturbances and it is obvious effective on optimizing the spatial wind field and reducing the concentration of salt fog. Besides, vortex flow of way one is obviously stronger and more concentrated than the other. Relatively, the vortex flow of way two is weaker than way one but wider scope [6]. The situation of way three is has the worst effect relatively.

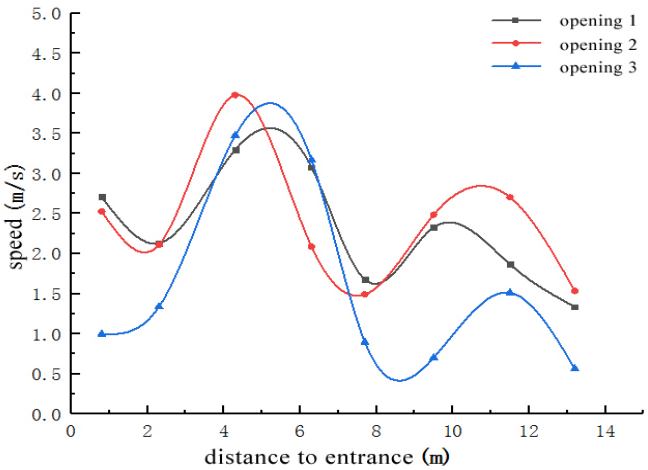

Figure 6. Air velocity distribution of three ways

As the Fig.6 and table 2 (point 1 is near the pressure inlet) show, way one: the wind speed varies from 1.5m/s to 4.0m/s; the peak is near the middle of the beam lattice side the longitudinal beam; the trough is near the pressure outlet of the rail beam. Way two: the whole trend is similar to the situation of no vents except the peak which is over 4m/s and the stability is not as good as the stability of way one. Way three: the wind speed is undulating and the minimum is below 0.5m/s. To sum up, the situation of way one and way two is similar and more stable. There is no obvious difference of the airflow between way three and the situation of no vents [7].

Table 2. Wind speed of characteristic points of the three ways

Points	1	2	3	4	5	6	7	8
Way one	2.7077	2.1305	3.3978	3.0773	1.7750	2.4290	2.0653	1.5355
Way two	2.5264	2.1157	4.0914	2.0866	1.5049	2.6155	3.0415	1.5365
Way three	1.0965	1.4377	3.6247	3.3686	0.8938	0.8021	1.6130	0.5619

For the high piled wharf, vents on the beam are effective on the salt mist dissipation. Besides, the pressure of certain space is also affected (Table 3, point 1 is near the inlet). The negative pressure of points 1, 2 & 3 (close to the inlet) is larger , including point 8 which is near the air outlet. However, the pressure of points 5, 6 & 7 is small away from the air inlet and outlet. The whole trend coincides well with the wind speed and conforms to the inference in Bernoulli's principle: the pressure is small if the flow rate is large.

Table 3. Air pressure distribution of beam lattice under different vents forms

Points	1	2	3	4	5	6	7	8
NO vents	8.99557	4.75056	6.59561	0.824681	2.25633	0.08117	2.67089	5.7506
Way one	25.8968	11.2497	14.4914	3.79329	1.96362	1.85542	2.98942	5.24799
Way two	24.5698	7.78055	19.2411	8.09769	4.12062	3.65248	3.66915	6.52655
Way three	19.7127	2.49853	11.3217	2.89005	1.23766	1.03769	0.67835	2.48261

Overall, the wind speed in the beam lattice of way one & two is larger than that of way three. The peak velocity of way two is over that of way one. The distribution of the wind speed of way three is instable [8]. Under the certain ventilation holes area and quantity, the pitch of way one & two is much larger than that of way three.

5. Conclusion

This paper studies the law of wind speed and pressure in the beam lattice with different forms of vents by establishing the three dimensional model of the high pile wharf with panel drains (concurrently exhaust). The conclusion is as follows:

Vents set on the longitudinal beams horizontally can greatly change the airflow distribution and relieve the structural corrosion caused by the concentration of salt fog in the space of the beam. The mean wind speed and pressure are 2.39 m/s, 2.44 m/s, 1.67 m/s and 8.44 Pa, 9.71 Pa, 5.23 Pa when the distance between vents and beams are 0.4m, 1.2m and 2.4m. The effect is improved significantly compared to the situation (1.55m/s & 3.99Pa) without vents. In all cases, the effect is the best when the distance is 1.2m.

The three ways of vents all cause local vortex airflow. When the distance are 0.4m & 1.2m, the airflow is stronger. Therefore, 1.2m is the relatively best position. It provides a certain theoretical basis for optimizing the vents.

Compared to traditional anticorrosion measures, setting vents can save cost and be easy to be constructed. It is a new method for anticorrosion of high pile wharf.

Acknowledgements
This work was supported by the National Natural Science Foundation of China [51679080 and 51379073]; the Scientific and Technology Project of Jiangsu Provincial Water Resources Department [2017030]; and sponsored by Qing Lan Project.

References
[1] Liu Shinian, Su Wei etc. Application of thermal spraying anticorrosive coating in atmospheric environment [J]. Journal of Xi'an University of Science and Technology, 2014,02: 72-76(in Chinese).
[2] Lujing, Wang Guanghua, Huang Lezhi etc. Research status of anti-corrosion coatings for cold spraying [J]. Surface technology, 2016, 09:88-94 (in Chinese).
[3] Jiang Zhengwu, Sun Zhenpin, Wang Peiming. Effect of silane on corrosion resistance of high performance concrete of sea workers [J]. China Harbour Engineering, 2005, 01: 26-30(in Chinese).
[4] Y JF, Jensen BBB, Nordkvist, M etc. CFD modelling of axial mixing in the intermediate and final rinses of cleaning-in-place procedures of straight pipes [J]. Journal of Food Engineering, 2017, 221: 95-105.
[5] Huang Hongtao. Simulation and analysis of VOCs concentration field in indoor air environment by CFD [D]. Shanghai Normal University, 2008(in Chinese).
[6] Wang Yoncheng. Flow field simulation analysis and structure optimization of Z shaped bend pipe based on CFD [J]. Hydraulic pneumatic and seal, 2014, 09: 29-32.
[7] Liu,Yuanchuan; Xiao,Qing; Incecik, Atilla,et al. Establishing a fully coupled CFD analysis tool for floating offshore wind turbines [J]. ENERGY & FUELS, 2012(112): 280-301.
[8] Tang,Z; Liu,Yj; Yuan,JP, et al. Study of the critical velocity in tunnels with longitudinal ventilation and spray systems [J]. Engineering, Civil, 2017(90): 139-147.